Nano Today 35 (2020) 100922

Contents lists available at ScienceDirect

Nano Today

journal homepage: www.elsevier.com/locate/nanotoday

Blood exposure to graphene oxide may cause anaphylactic death in non-human primates

Yunfeng Lin[a,1], Yu Zhang[b,c,1], Jiang Li[b,c,1], Huating Kong[b,c], Qinglong Yan[b,c], Jichao Zhang[b,c], Wei Li[b,c], Ning Ren[b,c], Yunzhi Cui[b,c], Tao Zhang[a], Xiaoxiao Cai[a], Qian Li[d], Aiguo Li[b,c], Jiye Shi[b,c], Lihua Wang[b,c], Ying Zhu[b,c,*], Chunhai Fan[d,**]

[a] State Key Laboratory of Oral Diseases, National Clinical Research Center for Oral Diseases, West China Hospital of Stomatology, Sichuan University, Chengdu 610041, China
[b] Bioimaging Center, Shanghai Synchrotron Radiation Facility, Zhangjiang Laboratory, Shanghai Advanced Research Institute, Chinese Academy of Sciences, Shanghai 201210, China
[c] Division of Physical Biology, CAS Key Laboratory of Interfacial Physics and Technology, Shanghai Institute of Applied Physics, Chinese Academy of Sciences, Shanghai 201800, China
[d] School of Chemistry and Chemical Engineering, Frontiers Science Center for Transformative Molecules, and Shanghai Key Laboratory for Nucleic Acids Chemistry and Nanomedicine, Institute of Molecular Medicine, Renji Hospital, School of Medicine, Shanghai Jiao Tong University, Shanghai 200240, China

ARTICLE INFO

Article history:
Received 8 March 2020
Received in revised form 29 June 2020
Accepted 1 July 2020
Available online 11 July 2020

Keywords:
Graphene oxide (GO)
Blood exposure
Non-human primates
Anaphylactic death
Immunoglobulin E
Severe lung injury

ABSTRACT

Toxicological evaluation of graphene oxide (GO) has been actively pursued under the context of large-scale industrial production and the potential for clinical translation. Nevertheless, the safety of GO remains largely debated, especially due to the lack of toxicological profile in higher mammals. Here we show that blood exposure to GO under the maximum safe starting dose may cause accidental death of mammals, including non-human primates (1 in 5 Macaca fascicularis and 7 in 121 mice), while remains general amenable in others. Elevated levels of immunoglobulin E and severe lung injury were found in dead animals, suggesting the GO-induced acute anaphylactic reactions. Noticeably, we did not observe anaphylactic reactions and deaths for two other carbon nanomaterials, including single-walled carbon nanotubes and nanodiamonds. This difference might arise from the long in-vivo circulating time of two-dimensional GO materials. This study thus highlights the urgent need to evaluate the hypersensitivity risks of graphene and other nanomaterials.

Introduction

Graphene oxide (GO) and its derivates are an emerging class of carbon nanomaterials (CNMs). Due to its unique two-dimensional (2D) structure, GO possesses outstanding features such as ultra-high surface area, rendering it a type of highly attractive materials for industrial applications. The increasing production and use of GO in industrial applications like optical/electronic circuitry [1], energy generation and storage [2,3], raise the chance of human exposure to GO. In the meanwhile, more recent efforts have also been devoted to biomedical applications including cancer diagnostics, drug delivery, and immunotherapy [4–8]. However, these demonstrations generally remain at the stage of fundamental research with limited clinical translation. One primary hurdle is the safety concern of in-vivo use of GO. Thus, there is an urgent call for evaluating the impact of GO on human health.

Extensive studies on the toxicology of GO have been performed, mostly at the level of in-vitro cells and small model animals. However, the conclusions often vary greatly or even contradict each other across the studies on differently leveled models with different administration doses. For example, the often-observed CNMs-induced oxidative stress in in-vitro cultured cells and zebrafish may be well tolerated by mice [4,9–16]. Moreover, the immune responses to same materials are also diverse among animal species [17]. Especially, the potential impacts of GO on human remain unexplored. Non-human primate studies may provide valuable information due to their close genetic and physiological relation-

* Corresponding author at: Bioimaging Center, Shanghai Synchrotron Radiation Facility, Zhangjiang Laboratory, Shanghai Advanced Research Institute, Chinese Academy of Sciences, Shanghai 201210, China.
** Corresponding author.
E-mail addresses: zhuying@zjlab.org.cn (Y. Zhu), fanchunhai@sjtu.edu.cn (C. Fan).
[1] These authors contributed equally to this work.

https://doi.org/10.1016/j.nantod.2020.100922

ship with human beings [18,19]. However, toxicological profile of GO in non-human primates is not available.

In the present study, we investigate the impacts of blood exposure to GOs on BALB/c mice and non-human primates (Macaca fasciculari) under the maximum safe starting dose. For comparison, we also studied the effects from two other CNMs with different morphologies, including one-dimensional (1D) single-walled carbon nanotubes (SWCNTs) and zero-dimensional (0D) nanodiamonds (NDs). The experimental design, including the GO exposure, blood test, and major organ analysis, is shown in Fig. 1b.

Methods

Materials

Large GO sheets were prepared from purified natural graphite by using a modified Hummer's method [20]. Then they were suspended in a 3:1 mixture of concentrated H_2SO_4/HNO_3 and sonicated in a water bath for 24 h at room temperature. The pH of GO solution was adjusted to neutral and subsequently dialyzed against MilliQ water for several days to remove residual salts. NaOH (6 mol/L) was added to the GO suspension and bath sonicated for about 4 h. The resulting solution was neutralized, and subsequently dialyzed against MilliQ water for three days to remove residual salts. The small GO sheets in the supernatant were isolated by centrifugation at 12,000 rpm for 30 min [8]. Further, to impart aqueous stability, the small GO solution was added with 6-armed PEG-NH_2 (SunBio, Cat. Nos. P6AM-10) and EDC·HCl for sonication at room temperature for 30 min. The resultant solution was kept stirring vigorously at room temperature overnight. Following dialysis against MilliQ water for one week to remove unbound six-armed PEG-NH_2, the GO-PEG with mean thickness of 1.1 nm and lateral dimension ranged from 20 to 80 nm (named GO in text) in the supernatant were isolated by centrifugation at 12,000 rpm for 30 min. The details for characterization were shown in Fig. 1a and Supplementary Table S1.The resluting GO with mean hydrated diameter of ~192 nm (by DLS analysis) and high O-content (31.9 %, by XPS analysis) exhibited excellent stability in all biological solutions tested including serum (Supplementary Fig. S3, S4).

NDs with individual sizes of 2−10 nm, which are synthesized by detonation techniques, were supplied by Gansu Gold Stone Nano. Material. Co. Ltd. (Gansu, China). The unique crystal profile of the NDs was confirmed using an automatic X-ray diffractometer equipped with CuKα (1.541 Å) radiation (40 kV, 40 mA). TEM images showed that the size of the majority of ND clusters was about 40−200 nm (Supplementary Fig. S7). The details for characterization have been described in our previous work [21].

Purified SWCNTs (purified HiPco, <5 wt% ash content) were purchased from Carbon Nanotechnologies. They were refluxed in a 3:1 mixture of concentrated H_2SO_4/HNO_3 in a water bath for 40–48 h at 80 °C [22]. The pH of SWCNT solution was adjusted to neutral and subsequently dialyzed against MilliQ water for several days to remove residual salts. Following 72-h sonication with Probe Sonicator, the shortened SWCNTs were conjugated with 6-armed PEG-NH_2 with the same method as mentioned above. SWCNT-PEG with length ~50−300 nm in the supernatant were isolated by centrifugation at 5000 rpm for 15 min. The details for characterization were shown in Supplementary Table S1 and Fig. S3.

Endotoxin was measured by a Limulus amebocyte lysate assay kit according to manufacturer's specifications (Associates of Cape Cod). The maximum sensitivity of this assay was 0.005 EU/mL. All CNMs were negative for endotoxin within this detection limit.

Cell lines and treatment

Cervical carcinoma HeLa cells and normal bronchial epithelial BEAS-2B cells were grown in RPMI1640 (Gibco) cell culture medium supplemented with 10 % fetal bovine serum (FBS). RAW264.7 macrophage-like cells were grown in the Dulbecco's modified Eagle's medium (DMEM) supplemented with 10 % FBS. The resultant cell suspensions (7×10^4 cells/mL for HeLa and BEAS-2B cells, 1×10^5 cells/mL for RAW264.7 cells) were dispensed into 24-well plates and incubated overnight to allow for cell adherence. After washing twice with phosphate buffered saline (PBS), cells were exposed to each CNM at required dose for 24 h.

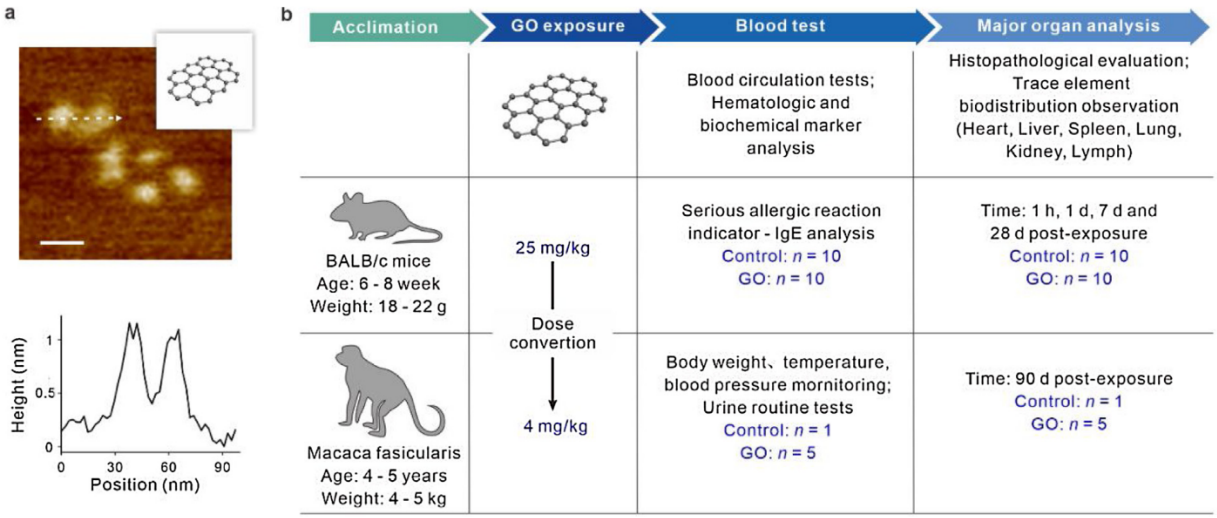

Fig. 1. Materials and experimental design. (a) AFM image of GO. Scale bar =50 nm. The experiments were repeated three times independently. (b) Experimental design. BALB/c mice were administered intravenously (i.v.) with normal saline (NS, 200 μL) or GO (25 mg/kg). n = 10 for each group. The evaluation system was composed of the following (1): blood circulation of GO, (2) hematologic and biomedical markers analysis at various time points, (3) major organ histopathological evaluation at 1, 7, 14 and 28 d post-administration, (4) trace element biodistribution observation at 28 d post-administration, (5) serious allergic reaction indicator detection at the initial 12 h after treatment. Macaca fascicularis were administered intravenously (i.v.) with NS (20 mL, n = 1) or GO (4 mg/kg, n = 5). The evaluation system was composed of the following: (1) blood circulation of GO; (2) hematologic, biomedical markers and urine routine analysis at various time points; (3) major organ histopathological evaluation at 90 d post-administration; (4) trace element biodistribution observation at 90 d post-administration; (5) temperature and pressure monitoring every week following injection; (6) body weight monitoring every week following injection.

Small animal models and treatment

The study was conducted at the Laboratory Animals Center of National Chengdu Center for Safety Evaluation of Drugs, Chengdu and all animal protocols were approved by the Institutional Animal Care and Use Committee of West China hospital, Sichuan University. BALB/c mice (male, 18∼22 g) were purchased from Shanghai SLAC Laboratory Animal Co. Ltd., China, and maintained under pathogen-free conditions according to American Association for Accreditation of Laboratory Animal Care (AAALAC) guidelines. Five in standard cages with free access to food and water and a 12-h light/dark cycle.

Groups of mice (n = 10 for each timepoint) were tail vein injected with CNM dispersions in 0.9 % sodium chloride as required. The evaluation system was composed of the following (1): blood circulation of each CNM, (2) hematologic and biomedical markers analysis at various time points, (3) major organ histopathological evaluation at 1, 7, 14 and 28 d post-administration, (4) trace element biodistribution observation at 28 d post-administration, (5) hypersensitive indicator detection at the initial 12 h after GO treatment. Before dissection, animals were anesthetized by 0.6 % pentobarbital sodium (i.p. 60 mg/kg).

Large animal models and treatment

The study was also conducted at the Laboratory Animals Center of National Chengdu Center for Safety Evaluation of Drugs, Chengdu, and all animal protocols were approved by the Institutional Animal Care and Use Committee of West China hospital, Sichuan University. Adult male Macaca fascicularis (n = 5 for each CNM and n = 1 for control) ranging from 4 to 5 years in age and from 3.9 to 5.1 kg in mass were reserve animals in this center. According to AAALAC guidelines, animals were individually housed in stainless steel cages (16–26 °C, 40–70% relative humidity, 12/12 h light/dark cycle, automatic control of a Honeywell central air-conditioning system) and fed a commercial monkey diet. Water was available ad libitum. Research staff inspected the monkeys two times each day. Eating fresh fruits twice a week and watching movies several times a week.

Groups of monkeys were administrated with CNM dispersions in 0.9 % sodium chloride via intravenous infusion (2 mL/min) as required. Based on the U. S. FDA Guidance, the mouse dose in mg/kg was converted to the monkey equivalent dose in mg/kg according to the following formula [23]:

$$HED^{a} = mousedoseinmg/kg \times (mouseweightinkg/humanweightinkg)^{0.33}$$

$$HED^{a} = monkeydoseinmg/kg \times (monkeyweightinkg/humanweightinkg)^{0.33}$$

(HED : humanequivalentdose; a : assumes60kghuman).

The evaluation system was composed of the following (1): blood circulation of each CNM, (2) hematologic, biomedical markers and urine routine analysis at various timepoints, (3) major organ histopathological evaluation at 90 d post-administration, (4) trace element biodistribution observation at 90 d post-administration, (5) temperature and pressure monitoring every week following injection. (6) body weight monitoring every week following injection. Before dissection, animals were anesthetized by 3% pentobarbital sodium (i.v. 30 mg/kg).

Results

The GO used in this study was synthesized as previously described. GO was further modified with six-arm branched polyethylene glycol (PEG) to increase its water dispersity and biocompatibility. [5] Atomic force microscope (AFM) images and TEM analysis (Fig. 1a and Supplementary Fig. S1, S2) showed that the GO structures were mostly single-layered sheets with a mean thickness of 1.1 nm and a size range of 20∼80 nm. Zeta potential measurements show that the GO is slightly negatively charged after PEGylation (Supplementary Table S1), generally in agreement with previous in-vivo studies.

We first assessed the cytotoxicity of the GO in cultured cell lines including carcinoma cells (HeLa cells), normal bronchial epithelial cells (BEAS-2B cells) and macrophage immune cells (RAW264.7 cells). The MTT assay results suggest that the maximal safe dose of GO for in-vitro cultured cells (cell viability >90 %) is ∼51 μg/mL (Supplementary Fig. S5a,b). Confocal microscopic imaging revealed that under this dose, GO (labeled with XenoLight CF770) was effectively internalized by these cells (Supplementary Fig. S5c, Fig. S6 and Table S1, S2). In comparison, NDs presented a higher max safe dose (∼52 μg/mL), while PEGylated SWCNTs presented a much lower one (1.5 μg/mL) (Supplementary Fig. S5a, b). These results suggest that the safe doses of CNMs have a dependency on their dimensions and shapes (Supplementary Fig. S6).

To determine proper dose of GO for non-human primates, we converted the maximum safe dose for BALB/c mice to the equivalent dose for Macaca fascicularis (i.e., maximum recommended starting dose, or MRSD) according to the guidance from U. S. Federal Drug and Food Administration (FDA) [23]. With consideration of the GO doses used in previous mice studies [24–26], we here chose 25 mg/kg as the max safe dose (or n̈o observed adverse effect level¨) of PEGylated GO for mice. Thus, after the conversion based on normalization of dose to body surface area (detailed in Method section), the MRSD of GO for Macaca fascicularis is 4 mg/kg. Likewise, we derived that the MRSDs of SWCNTs and NDs for Macaca fascicularis are 4 mg/kg and 0.12 mg/kg, respectively.

In the animal tests (Supplementary Table S3, S4), the GO suspended in 0.9 % sodium chloride was administrated with the MRSD, via tail vein injection for mice or intravenous infusion for monkeys. To our surprise, 7 out of the 121 treated mice died 1∼12 h post GO exposure (mortality rate 5.8 %, Fig. 2a and Supplementary Table S5). We observed that at least one mouse suffered hematemesis before its death (Supplementary Fig. S8). As for the Macaca fasciculari, one out of the 5 monkeys died ∼1.5 h post GO exposure (morality rate 20 %). Before its death, this monkey squatted on the ground with a painful expression (seemingly thoracic pain) and hematemesis. In comparison, ND or SWCNT treatments under their MRSD separately did not cause any hematemesis or death of the animals (Supplementary Fig. S9).

To find out the cause of death, we first performed blood tests in the GO-treated animals. We sampled and examined the blood from the survived mice at different time points (1, 2, 6, and 12 h, 5 mice for each time point, respectively) post GO exposure. We observed that 5 out of the 20 mice (25 %) exhibited abnormal levels of indicators, which include two hepatic function indicators – aspartate transaminase (AST) and alanine transaminase (ALT), and two cardiac indicators – creatine kinase (CK) and lactate dehydrogenase (LDH) (Fig. 2b and Supplementary Fig. S9). These indicators rose by approximately 3–20 folds in these mice compared to the average levels of the control group (mice untreated with GO). Especially, the CK level exhibited a rapid rise (4-fold rise in the first hour post-exposure) (Fig. 2b). These abnormal indicators suggest that acute and severe liver and heart injury occurred in these animals. As for the dead monkey, the levels of AST, ALT, CK and LDH prior to its death also rose by approximately 8, 20, 10, and 21 folds, respectively, compared to the control group (Fig. 2c). These results suggest that there might be anaphylactic reactions (or hypersensitivity reactions) in these GO-treated animals. Anaphylaxis is a severe, life-threatening hypersensitivity reaction (HSR) initiated by exposure to a specific antigen in a sensitized organism. It usually occurs within minutes to hours of exposure, and is typically

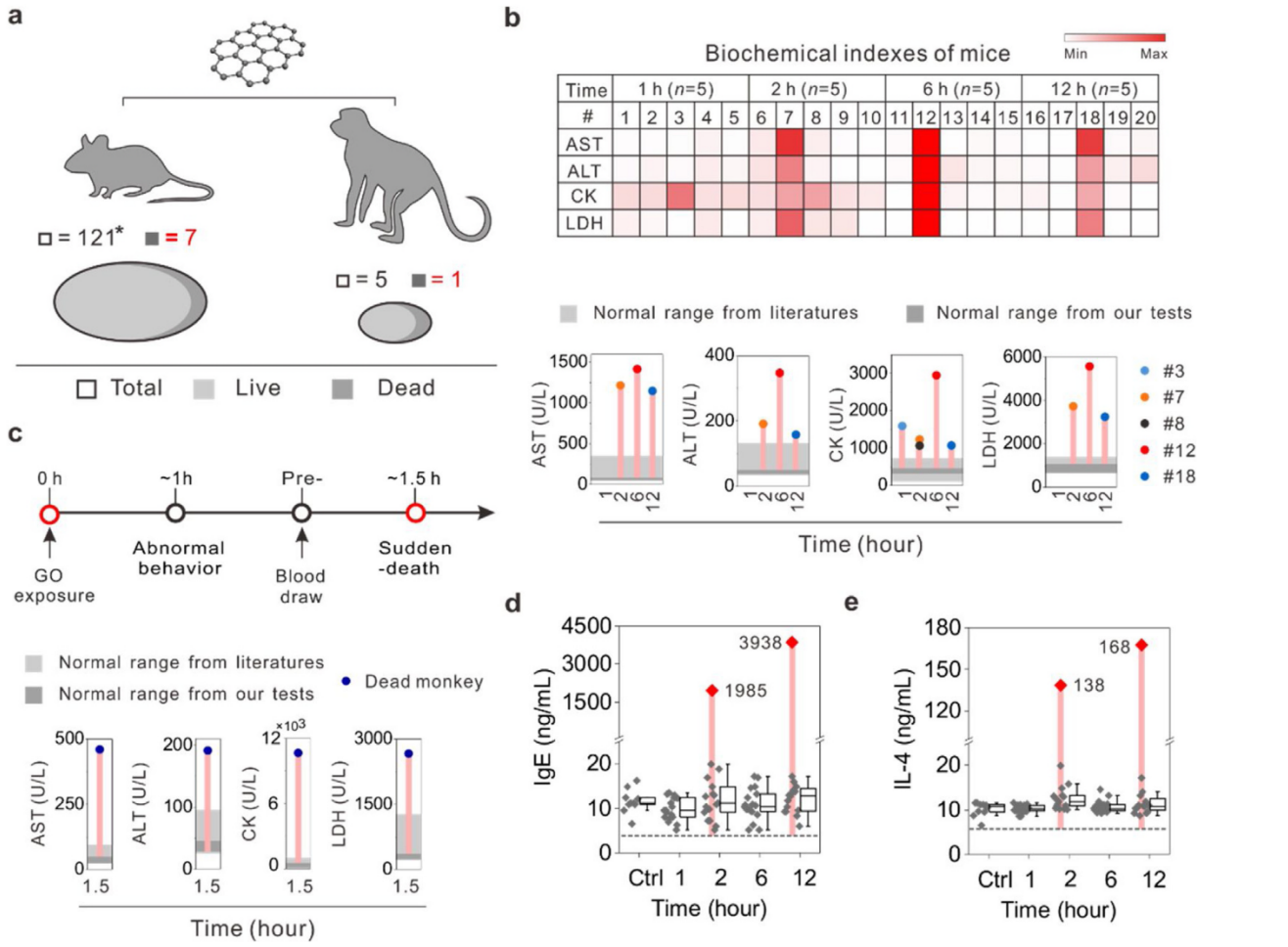

Fig. 2. GO induced anaphylactic reactions in murines and non-human primates. (a-c) Animals were administered intravenously (i.v.) with GO as indicated in Fig.1. (a) The numbers of live and sudden-death animals after GO administration. *Due to the sudden-death of mice after GO treatment, the animal number of this group was increased to 121 to make sure that there were enough animals for diverse tests at each timepoint. (b, c) Abnormal biochemical indexes of treated mice (b) and monkeys (c). b upper: Biochemical indexes of mice showed by indicated colors. The range of index level noted by the color bar is 58 - 1402 U/L for AST, 42 - 337 U/L for ALT, 137 - 2861 U/L for CK and 654 – 5500 U/L for LDH. c upper: Schematic showing of one monkey died at ~1.5 h post GO exposure. The region rendered in light gray represents the normal range from the literature (Supplementary Table S6), and the dark gray region represents the range observed in mice without any treatment (Supplementary Table S7). (d, e) BALB/c mice were administered intravenously (i.v.) with normal saline (NS, 200 μL) or GO (25 mg/kg). Blood samples were collected 1 - 12 h post GO exposure, and serum IgE (d) and IL-4 (e) levels were analyzed with ELISA. Due to the sudden-death of mice after GO exposure, the animal number for serum IgE/IL-4 analysis was 19, 17, 19 and 16 at 1, 2, 6 and 12 h, respectively. Data are represented as means ± SD. Light red rectangular columns in (b – e) indicate dramatic rises in tested biochemical indexes.

associated with sudden rise of certain hepatic/cardiac indicators [27–29]. It is worth noting that among the mice the incidence of having abnormal indicators (25 %) was much higher than the death rate (5.8 %), suggesting that the mice may suffer but survive this abnormal condition. Moreover, the indicators from all survived GO-treated monkeys were within the normal range, suggesting that the monkeys might have lower tolerance to the GO-induced anaphylactic reaction compared to the mice under the equivalent dose.

Given that anaphylaxis is typically mediated by immunoglobulin E (IgE) antibodies (or so called Type I HSR) [30–34], we measured the serum IgE level and representative T helper type 2 (T_H2) cytokine interleukin 4 (IL-4) level in the GO-treated mice. We observed that in 71 mice (survived the GO exposure until blood collection), two (i.e., 2.8 %) exhibited abnormally elevated IgE/IL-4 level compared to the control group. One of them showed 180/13-fold rise in IgE/IL-4 level 2 h after the GO exposure, and the other showed 340/16-fold rise 12 h after the exposure (Fig. 2d, e), indicating that GO induce T_H2-IgE responses in mice via IL-4 production [35,36]. Considering that the IgE levels of mice dead from GO exposure were not obtained. The actual incidence of IgE elevation may be higher than 2.8 % here. Additionally, we in this study employed PEGylated GO, and its the average hydrodynamic size in all biological solutions tested including serum is almost the same (Supplementary Fig. S4), which indicates that PEGylation completely prevents protein adsorption, thereby preventing the activation of complement system [37].These data confirmed the speculation that GO may induce IgE-mediated anaphylactic reaction in mammals. In future, further research such as the contribution of basophils to the T_H2-IgE response in vitro and in vivo through the production of IL-4 [35,36] is needed to better support our proposed mechanism of anaphylaxis for GO

We next studied the blood circulation of GO in the animals. The GO was labeled with XenoLight CF770. The fluorescence of blood collected from the animals was measured using a small animal optical imaging system. We found that in mice, the GO presented an average plasma half-life of ~5 h (Fig. 3a and Supplementary Fig. S12, S13). In comparison, NDs and SWCNTs showed much shorter half-lives (~20 min and 2 h, respectively). In monkeys, the plasma half-life of GOs was ~40 h, while which of NDs and SWCNTs were ~79 min and ~4 h, respectively (Fig. 3b and Supplementary Fig. S14). Overall, the GO presented the longest half-time among the

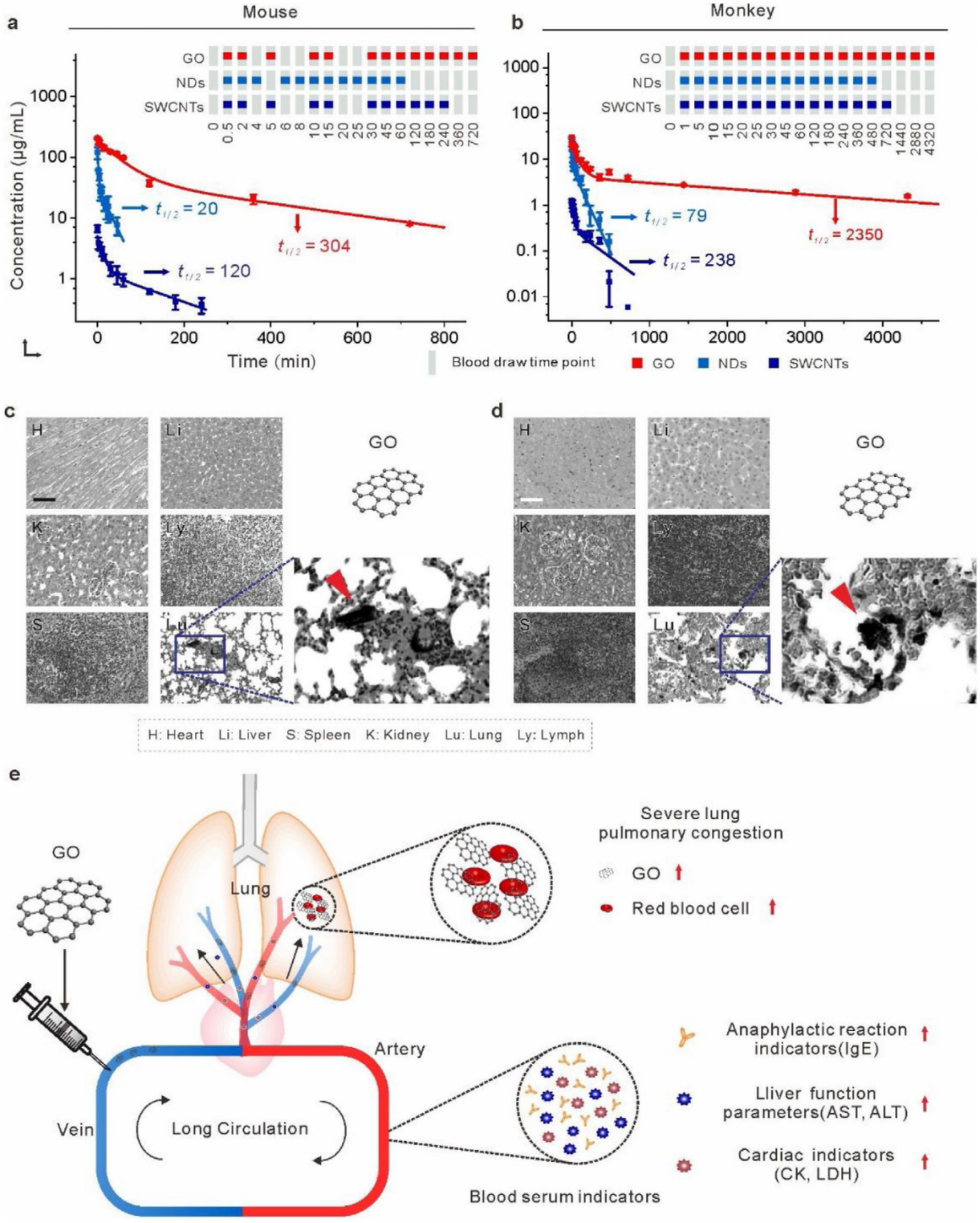

Fig. 3. Analysis of GO-induced cross-species anaphylactic reactions. (a, b) Blood circulation curves of the CNMs in mice (a) or monkeys (b), determined by CF770 fluorescence in the blood at different time points post injection (n = 3). (c, d) Histological images from the major organs of the dead (c) mouse and (d) monkey after GO treatment. Images were taken at ×40 magnification with standard haematoxylin and eosin staining. Fine granular black pigment in the lung tissues (likely to be GO) is indicated with arrows. Scale bar =50 μm. Color images are provided in Supplementary Fig. S15a (mice) and Fig. S16a (monkeys), respectively. (e) Schematic overview of GO-induced cross-species anaphylactic reactions. Long circulation of GO in blood induced anaphylactic reaction, resulting in increase of some certain biochemical markers, associated with severe lung pulmonary congestion, eventually even led to sudden death.

three CNMs. Moreover, the half-time of GO in the monkey was much longer than that in mice. These results suggest that the GO-triggered anaphylactic reactions might arise from the long blood circulation time of GO.

We excised and examined the major organs of the animals dead from GO exposure (the dead monkey and one of the dead mice). In the histological images, we found that the lung parenchyma presented severe structural damage to alveolar. A large number of red

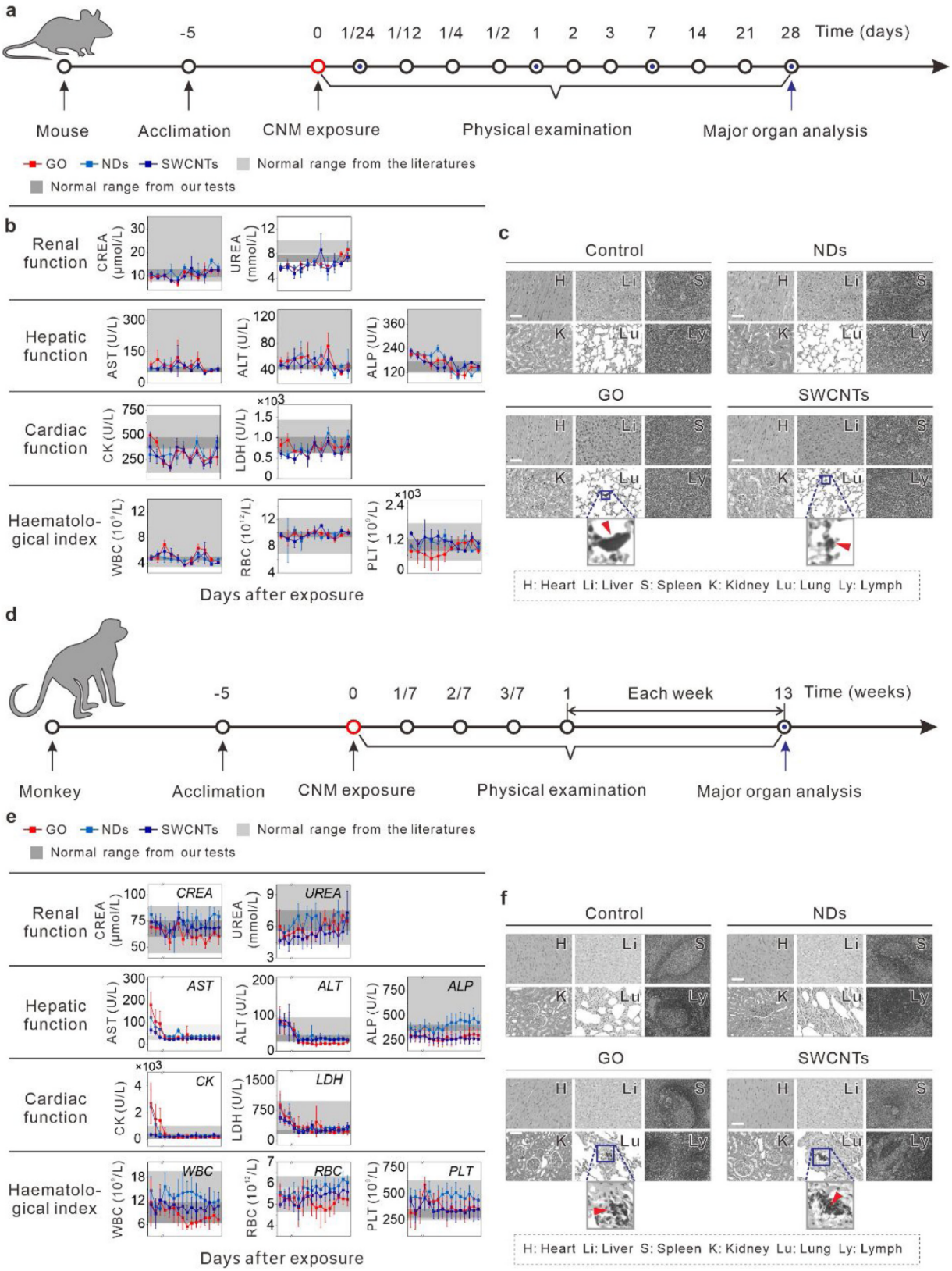

Fig. 4. Biocompatibility assessment of three types of CNMs in murines and non-human primates. (a-c) BALB/c mice were administered intravenously (i.v.) with normal saline (NS, 200 μL), NDs (25 mg/kg), GO (25 mg/kg) or SWCNTs (0.75 mg/kg). (d-f) Macaca fascicularis were administered intravenously (i.v.) with NS (20 mL, n = 1), NDs (4 mg/kg, n = 5), GO (4 mg/kg, n = 5) or SWCNTs (0.12 mg/kg, n = 5). (a,d) Experimental design. (b,e) Blood test results of (b) treated mice (In GO exposure groups, n = 4 for AST 2, 6, 12 h, ALT 2, 6, 12 h, CK 1, 6, 12 h, LDH 2, 6, 12 h and n = 3 for CK 2 h. In other groups, n = 5) and (e) treated monkeys (In GO exposure groups, n = 4. In other groups, n = 5). The region rendered in light gray represents the normal range from the literature (Supplementary Table S6), and the dark gray region represents the range observed in mice without any treatment (Supplementary Table S7). Error bars represent one standard deviation above or below the mean. Abbreviations: aspartate transaminase, AST; alanine transaminase, ALT; alkaline phosphatase, ALP; creatinine, CREA; creatine kinase, CK; lactic dehydrogenase, LDH; white blood cell count, WBC; red blood cell count, RBC;

blood cells seeped into alveolar cavities, indicating diffuse alveolar hemorrhage (Fig. 3c, d and Supplementary Fig. S15a, S16a). We also observed granular black pigment seemingly GO in the pulmonary parenchyma. Additional Raman spectral scan of the granular black pigment evidenced it (Supplementary Fig. S15b, S16b). In contrast, samples of heart, liver, spleen, kidney and lymph from the dead animals exhibited no obvious changes. Thus, we reason that maybe the long circulation of GO in blood leads to its distal retention and deposition in the lung tissue, which can induce anaphylactic reactions there, resulting in deadly pulmonary congestion (Fig. 3e).

Apart from the GO-triggered anaphylactic reactions, however, all the three CNMs including GO in this study (Fig. 4a, d and Supplementary Table S3, S4) show minimum adverse effects in the animals under their MRSD. All examined indicators from blood and urine of the CNMs-treated mice (Fig. 4b and Supplementary Table S6, S7, Fig. S9) or monkeys (Fig.4e and Supplementary Table S6-S22, Fig. S11) fell in the normal range throughout the examination period, suggesting that the CNMs did not cause acute toxicity or liver/kidney/heart injuries to these animals. To further evaluate the long-term effects of the CNM blood exposure, we performed histological analysis of tissues from the mice 28 days post-exposure or the monkeys 90 days post-exposure. We found that except for those suffered anaphylactic reactions, all the animals showed little pathological changes in their major organs including heart, liver, spleen, kidney, lung and lymph. (Fig. 4c for mice and Fig. 4f for monkeys, detailed in Supplementary Fig. S17, S18). Synchrotron-based X-ray fluorescence (XRF) mapping of several trace elements (including Fe, Cu, Zn, K, Ca, Cl and S) in the major organs of CNMs-treated animals also indicates that there was no abnormality in the biodistribution of these essential elements (Supplementary Fig. S19-S30) [38]. Throughout the entire study, we observed no behavioral abnormality among the mice or monkeys (Supplementary Fig. S31-S33).

It is worth noting that at certain time points, the mice or monkeys exposed to GO or SWCNTs had small amounts of granular black pigments seemingly CNM deposits in their lung or spleen (Fig. 4c, f and Supplementary Fig. S34, S35), indicating that these two CNMs can be retained in body tissues for days or even weeks. However, the CNM deposition does not necessarily induce anaphylactic reactions. In comparison, we found that NDs in mice could be cleared in all organs within one week (Fig. 4c and Supplementary Fig. S36), suggesting that NDs present less risk in triggering anaphylactic reactions.

Discussions

It is well established that the biological properties of nanomaterials are highly dependent on their structural parameters and surface chemical/physical properties. Previous studies have shown that nanomaterials with different sizes and shapes have dramatic differences in affinity to serum proteins, in vivo blood circulation time, distribution and retention, which can lead to different bioeffects [39–41]. In this study, we show that CNMs with different morphologies exert different impacts in animals. Blood exposure of the 2D GO materials might induce anaphylactic reactions in mice and non-human primates. In contrast, the particle-like (0D) ND structures and the needle-like (1D) SWCNT structures did not show such effect. This difference might be attributed to unique physicochemical properties of nanoscale GO including its large surface area and superior stability in physiological environment [42] (Supplementary Fig. S4), which lead to long blood circulation time of GO in vivo. Given that it remains challenging to obtain monodisperse CNMs with precise size and shape, it is reasonable that the conclusions from toxicology studies on a same kind of CNMs often vary or even contradict each other. Thus, for in-vivo applications, nanomaterials of the same kind yet with different sizes and shapes should still be considered as distinct materials and undergo comprehensive toxicology evaluation.

Our study also calls the attention that simple conversion of the equivalent GO dose from other species cannot ensure the safety of human, due to the diversity of metabolic rates and immune responses across different species and individuals. Previous reports have shown that the doses required to induce hypersensitivity reactions in mice and rats are several orders of magnitude higher than those needed to trigger reactions in humans [43]. Non-human primate, can reproduce clinical symptoms of human patients, thus is suitable for preclinical safety studies. We demonstrate that the mice possess faster metabolic rate and higher tolerance of GO compared to the monkeys, suggesting that in-vivo applications of nanomaterials in higher mammals should receive more attention. Especially, individual allergy tests and screening anaphylaxis antagonists as auxiliary means are necessary prior to the human trial of GO and GO derivates. Considering the individual diversity in GO sensitivity, the MRSD of GO should be set to a lower level than expected.

Taken together, we demonstrate that the blood exposure of GO under the MRSD may induce anaphylactic death in non-human primates. As compared to other CNMs including SWCNTs and NDs, GO has longer blood circulation time. Although GO shows no acute or long-term adverse effects in most mice or monkeys, the non-neglectable anaphylactic reactions and even death induced by GO raise concerns on their in-vivo safety. This study thus suggests that case-by-case allergy tests are indispensable prior to the biomedical use of nanomaterials.

Declaration of Competing Interest

The authors declare that they have no known competing financial interests or personal relationships that could have appeared to influence the work reported in this paper.

Acknowledgments

This work was supported by the National Key Research and Development Program (2016YFA0400900), the National Natural Science Foundation of China (11675251, 21834007, 21775157, 21675167, 81970916, 81671031), the Key Research Program of Frontier Sciences (QYZDJ-SSW-SLH031), the Open Large Infrastructure Research of CAS, LU Jiaxi International Team of the Chinese Academy of Sciences, the Innovative research team of high-level local universities in Shanghai, and the K.C. Wong Foundation at Shanghai Jiao Tong University.

Appendix A. Supplementary data

Supplementary material related to this article can be found, in the online version, at doi:https://doi.org/10.1016/j.nantod.2020.100922.

platelet count, PLT. (c,f) Histological images from the major organs of the mice (c) at 28 d post-exposure and the monkeys (f) at 90 d post-exposure. Tissues were collected from heart, liver, spleen, kidney, lung and lymph. Images were taken at ×40 magnification with standard haematoxylin and eosin staining. Finely granular black pigment in the lung tissues (likely to be GO or SWCNTs) is indicated with red arrows. Scale bar =50 μm. Color images are provided in Supplementary Fig. S17 (mice) and Fig. S18 (monkeys), respectively.

References

[1] M.P. Levendorf, C.J. Kim, L. Brown, P.Y. Huang, R.W. Havener, D.A. Muller, J. Park Nature 488 (2012) 627–632.
[2] R. Raccichini, A. Varzi, S. Passerini, B. Scrosati, Nat. Mater. 14 (2015) 271–279.
[3] M.F. El-Kady, V. Strong, S. Dubin, R.B. Kaner, Science 335 (2012) 1326–1330.
[4] H.Y. Mao, S. Laurent, W. Chen, O. Akhavan, M. Imani, A.A. Ashkarran, M. Mahmoudi, Chem. Rev. 113 (2013) 3407–3424.
[5] K. Yang, S.A. Zhang, G.X. Zhang, X.M. Sun, S.T. Lee, Z.A. Liu, Nano Lett. 10 (2010) 3318–3323.
[6] H.J. Yoon, T.H. Kim, Z. Zhang, E. Azizi, T.M. Pham, C. Paoletti, J. Lin, N. Ramnath, M.S. Wicha, D.F. Hayes, D.M. Simeone, S. Nagrath, Nat. Nanotechnol. 8 (2013) 735–741.
[7] R.K. Thapa, J.H. Byeon, S.K. Ku, C.S. Yong, J.O. Kim, NPG Asia Mater. 9 (2017).
[8] Z. Liu, J.T. Robinson, X.M. Sun, H.J. Dai, J. Am. Chem. Soc. 130 (2008) 10876–10877.
[9] V.N. Mochalin, O. Shenderova, D. Ho, Y. Gogotsi, Nat. Nanotechnol. 7 (2012) 11–23.
[10] K. Kostarelos, A. Bianco, M. Prato, Nat. Nanotechnol. 4 (2009) 627–633.
[11] Z. Liu, S. Tabakman, K. Welsher, H.J. Dai, Nano Res. 2 (2009) 85–120.
[12] R.H. Hurt, M. Monthioux, A. Kane, Carbon 44 (2006) 1028–1033.
[13] N. Dworak, M. Wnuk, J. Zebrowski, G. Bartosz, A. Lewinska, Carbon 68 (2014) 763–776.
[14] M. Zheng, J.G. Lu, G.M. Lin, H.L. Su, J.Y. Sun, T.G. Luan, Environ. Pollut. 254 (2019) 112969.
[15] P.P. Jia, T. Sun, M. Junaid, L. Yang, Y.B. Ma, Z.S. Cui, D.P. Wei, H.F. Shi, D.S. Pei, Environ. Pollut. 247 (2019) 595–606.
[16] A.C. Barrios, Y. Wang, L.M. Gilbertson, F. Perreault, Environ. Sci. Technol. 53 (2019) 14679–14687.
[17] M.A. Dobrovolskaia, S.E. Mcneil, Nat. Nanotechnol. 2 (2007) 469–478.
[18] R.W. Myers, H.P. Guan, J. Ehrhart, A. Petrov, S. Prahalada, E. Tozzo, X.D. Yang, M.M. Kurtz, M. Trujillo, D.G. Trotter, D.Q. Feng, S.Y. Xu, G. Eiermann, M.A. Holahan, D. Rubins, S. Conarello, X.D. Niu, S.C. Souza, C. Miller, J.Q. Liu, K. Lu, W. Feng, Y. Li, R.E. Painter, J.A. Milligan, H.B. He, F. Liu, A. Ogawa, D. Wisniewski, R.J. Rohm, L.Y. Wang, M. Bunzel, Y. Qian, W. Zhu, H.W. Wang, B. Bennet, L.L. Scheuch, G.E. Fernandez, C. Li, M. Klimas, G.C. Zhou, M. van Heek, T. Biftu, A. Weber, D.E. Kelley, N. Thornberry, M.D. Erion, D.M. Kemp, I.K. Sebhat, Science 357 (2017) 507–511.
[19] T. Nakamura, I. Okamoto, K. Sasaki, Y. Yabuta, C. Iwatani, H. Tsuchiya, Y. Seita, S. Nakamura, T. Yamamoto, M. Saitou, Nature 537 (2016) 57–62.
[20] W.S. Hummers, R.E. Offeman, J. Am. Chem. Soc. 80 (1958), 1339-1339.
[21] Y. Zhang, Z.F. Cui, H.T. Kong, K. Xia, L. Pan, J. Li, Y.H. Sun, J.Y. Shi, L.H. Wang, Y. Zhu, C.H. Fan, Adv. Mater. 28 (2016) 2699–2708.
[22] J. Liu, A.G. Rinzler, H.J. Dai, J.H. Hafner, R.K. Bradley, P.J. Boul, A. Lu, T. Iverson, K. Shelimov, C.B. Huffman, F. Rodriguez-Macias, Y.S. Shon, T.R. Lee, D.T. Colbert, R.E. Smalley, Science 280 (1998) 1253–1256.
[23] Guidance for Industry: Estimating the Maximum Safe Starting Dose in Initial Clinical Trials for Therapeutics in Adult Healthy Volunteers, U.S. Department of Health and Human Services, Food and Drug Administration, Center for Drug Evaluation and Research (CDER), 2005.
[24] S.L. Liang, S. Xu, D. Zhang, J.M. He, M.Q. Chu, Nanotoxicology 9 (2015) 92–105.
[25] S. Xu, Z.Y. Zhang, M.Q. Chu, Biomaterials 54 (2015) 188–200.
[26] W. Miao, G. Shim, S. Lee, S. Lee, Y.S. Choe, Y.K. Oh, Biomaterials 34 (2013) 3402–3410.
[27] D. Bani, S. Nistri, P.F. Mannaioni, E. Masini, Curr. Allergy Asthma R. 6 (2006) 14–19.
[28] X.J. Tang, B.L. Que, X.R. Song, S.H. Li, X.J. Yang, H.L. Wang, H.L. Huang, M. Kamijima, T. Nakajima, Y.C. Lin, L.Y. Li, J. Occup. Health 50 (2008) 114–121.
[29] R.S. Scalco, S. Chatfield, M.H. Junejo, S. Booth, J. Pattni, R. Godfrey, R. Quinlivan, Am. J. Case Rep. 17 (2016) 905–908.
[30] T.T. Hansel, H. Kropshofer, T. Singer, J.A. Mitchell, A.J.T. George, Nat. Rev. Drug Discov. 9 (2010) 325–338.
[31] P. Lieberman, S.F. Kemp, J. Oppenheimer, D.M. Lang, I.L. Bernstein, R.A. Nicklas, J.A. Anderson, J.I. Bernstein, J.N. Fink, P.A. Greenberger, D.K. Ledford, J. Li, A.L. Sheffer, R. Solensky, B.L. Wolf, J. Allergy Clin. Immunol. 115 (suppl) (2005) S485–523.
[32] S.J. Galli, M. Tsai, Nat. Med. 18 (2012) 693–704.
[33] J. Ring, M. Grosber, M. Mohrenschlager, K. Brockow, Chem. Immunol. Allergy 95 (2010) 201–210.
[34] T. Ishizaka, K. Ishizaka, Prog. Allergy 19 (1975) 60–121.
[35] T. Yoshimoto, K. Yasuda, H. Tanaka, M. Nakahira, Y. Imai, Y. Fujimori, K. Nakanishi, Nat. Immunol. 10 (2009) 706–712.
[36] H.Y. Kim, R.H. DeKruyff, D.T. Umetsu, Nat. Immunol. 11 (2010) 577–584.
[37] S.P. Mukherjee, M. Bottini, B. Fadeel, Front. Immunol. 8 (2017) 673.
[38] L.A. Finney, T.V. O'Halloran, Science 300 (2003) 931–936.
[39] C. Kinnear, T.L. Moore, L. Rodriguez-Lorenzo, B. Rothen-Rutishauser, A. Petri-Fink, Chem. Rev. 117 (2017) 11476–11521.
[40] Y. Geng, P. Dalhaimer, S.S. Cai, R. Tsai, M. Tewari, T. Minko, D.E. Discher, Nat. Nanotechnol. 2 (2007) 249–255.
[41] Y.C. Wei, L. Quan, C. Zhou, Q.Q. Zhan, Nanomedicine-UK 13 (2018) 1495–1512.
[42] D. Bitounis, H. Ali-Boucetta, B.H. Hong, D.H. Min, K. Kostarelos, Adv. Mater. 25 (2013) 2258–2268.
[43] J. Szebeni, D. Simberg, A. Gonzalez-Fernandez, Y. Barenholz, M.A. Dobrovolskaia, Nat. Nanotechnol. 13 (2018) 1100–1108.

Yunfeng Lin obtains his B.S. and Ph.D. degree from Sichuan University in 2001 and 2006. He joined the West China College of Stomatology, Sichuan University at 2006 and became the full professor of Sichuan University since 2008. He took his postdoctoral research at Harvard University between 2009 and 2010. He is Vice-director of West China Medical Center, Sichuan University and Vice-director of State Key Laboratory of Oral Diseases. His main research focus on stem cell biology, DNA nanomaterial and tissue regeneration.

Yu Zhang obtained her B.S. degree from Shihezi University in 2009. She obtained her Ph.D. degree from Shanghai Institute of Applied Physics, Chinese Academy of Sciences (SINAP, CAS), in 2016 and took her postdoctoral research there. Now she is an assistant professor of the Bioimaging Center, Zhangjiang Laboratory, Shanghai Advanced Research Institute, CAS. Her research interests are functionalization and biological application of nanomaterials.

Jiang Li obtained his B.S. and Ph.D. degree from Sichuan University in 2003 and 2009, and joined the faculty at Shanghai Institute of Applied Physics, Chinese Academy of Sciences (SINAP, CAS) (2009–2018). Now he is an associate professor of the Bioimaging Center, Zhangjiang Laboratory, Shanghai Advanced Research Institute, CAS. His research interests are in developing DNA nanotechnology-empowered nanoprobes and cell imaging strategies.

Ying Zhu obtained her B.S. degree from Nanjing Normal University. She obtained her Ph.D. degree from Shanghai Institute of Applied Physics, Chinese Academy of Sciences (SINAP, CAS), in 2008, and joined the faculty at SINAP, CAS (2008–2018). Now she is a professor of the Bioimaging Center, Zhangjiang Laboratory, Shanghai Advanced Research Institute, CAS. Her research interests focus on synchrotron-based X-ray microscopy for bioimaging.

Chunhai Fan obtained his B.S. and Ph.D. degree from Nanjing University in 1996 and 2000. After his postdoctoral research at the University of California, Santa Barbara, he joined the faculty at Shanghai Institute of Applied Physics, Chinese Academy of Sciences, in 2004. In 2018, he became a SJTU Chair Professor at Shanghai Jiao Tong University. His research interests include biosensors, biophotonics, DNA nanotechnology and DNA computation.